TEM Study of the Misfit Intercalation Compounds α-$Hg_{1.19}TaS_2$ and β-$Hg_{1.3}TaS_2$

P. Moreau, P. Ganal, A. M. Marie, and G. Ouvrard*

Institut des Matériaux de Nantes, 2 rue de la Houssinière, 44072 Nantes, France

Received April 14, 1995[⊗]

Transmission electron microscopy has been employed to study the in-plane structure of intercalated Hg guest layers in the stage 1 misfit intercalation compounds α-$Hg_{1.19}TaS_2$ and β-$Hg_{1.3}TaS_2$. Both phases are remarkable for their complex composite crystal structures and for the very different Hg guest layer structures that they exhibit in spite of their similar Hg uptakes. Micro diffraction patterns of α-$Hg_{1.19}TaS_2$ suggest a chainlike Hg arrangement. Each Hg atom is surrounded by two nearest neighbor atoms at 2.78 Å and four next nearest neighbors at 3.2 Å. The Hg chains form an ordered sublattice that shares two commensurate axes with the TaS_2 host matrix (**a** and **c** axes) but is incommensurate along the Hg chain direction (**b** axis). In the case of β-$Hg_{1.3}TaS_2$, hexagonal close-packed Hg layers are formed. Here each Hg atom encounters six nearest neighbors at a 2.9 Å distance. The Hg sublattice is rotated by about 30° with respect to the TaS_2 host lattice. Thus, the total structure falls close to commensurability: the TaS_2 host layers can be viewed as a 2 × 2 superstructure built upon the hexagonal closed packed Hg layers. The Hg arrangements observed in α-$Hg_{1.19}TaS_2$ and β-$Hg_{1.3}TaS_2$ bear a strong resemblance to the (101) lattice planes in solid state β-Hg and the hexagonal Hg layers in Hg_3MF_6 (M = Ta, Nb), respectively. This analogy allows us to draw some instructive conclusions about the presence of the Hg metal bonding and its influence on the resulting crystal structures.

Introduction

Recent progress in theoretical description and in experimental precision has attracted considerable interest in the study of composite crystals.[1,2] These compounds are composed of two or more interpenetrating subsystems which are incommensurate along at least one crystallographic axis. The misfit between the two subsystems is, according to standard theories, the result of competing building principles and the fact that the intrasubset interaction dominates over the interaction between the subsets.[2,3]

An elegant way to test this idea is provided by intercalation chemistry. The intercalation of different guest species into low-dimensional materials such as graphite or the transition metal dichalcogenides (TMD) offers the possibility of tailoring the guest−guest as well as the guest−host interactions and, thus, of studying their effects on the resulting crystal structures.

The intercalation of guest species is in many cases accompanied by a significant charge transfer between the guest and the host system.[4] Because of the resulting Coulombic interaction, commensurate superstructures are usually formed and the guest atoms or molecules reside on specific crystallographic sites within the expanded host matrix.[5,6] For some graphite intercalation compounds (GIC), e.g. the high-stage alkali metal GIC and those formed with halides, discommensurate domain (DC) structures have been observed.[7,8] These structures can be considered as an intermediate case located between the ordinary (commensurate) intercalation compounds and the more complicated misfit layer compounds. In DC structures the intercalant resides, as for ordinary intercalation compounds, on specific lattice sites, forming locally commensurate guest islands. However, the commensurate guest islands are separated by discommensurate phase shifts which occur periodically at the domain boundaries.

Although quite a few misfit intercalation compounds have been reported in the past,[9−11] it was only recently that, with $Hg_{1.24}TiS_2$, the average structure of the first misfit intercalation compound was resolved.[12,13]

In this article we will report the in-plane Hg arrangements realized in the related stage 1 misfit intercalation compounds α-$Hg_{1.19}TaS_2$ and β-$Hg_{1.3}TaS_2$ as determined by transmission electron microscopy (TEM). Unlike Hg_xTiS_2, where only a chainlike Hg arrangement is seen, both chainlike and hexagonal Hg structures are possible in the TaS_2 van der Waals (vdW) gap. The intercalated Hg layers bear, with respect to symmetry and bond lengths, a strong resemblance to the (101) lattice planes in solid β-Hg and the hexagonal Hg layers in Hg_3MF_6 (M = Ta, Nb), respectively.[14,15] The implications of this analogy and its relation to the observed composite crystal structures will be discussed.

Experimental Section

Pure stage 1 α-$Hg_{1.19}TaS_2$ and β-$Hg_{1.3}TaS_2$ samples were prepared by direct reaction of TaS_2 and triply distilled Hg (<5 ppm of foreign metals). The mercury intercalation into 2H-TaS_2 was usually carried out at ambient temperature, whereas for 1T-TaS_2 an elevated reaction temperature of 423 K was necessary.[16,17] The TaS_2 host materials were prepared by a reaction involving iodine vapor transport from 99.95%

[⊗] Abstract published in *Advance ACS Abstracts,* October 1, 1995.

(1) Janssen, T.; Janner, A. *Adv. Phys.* **1987**, *36*, 519.
(2) Van Smaalen, S. Submitted to *Crystallogr. Rev.*
(3) Bak, P. *Rep. Prog. Phys.* **1982**, *45*, 587.
(4) Rouxel, J. In *Intercalated Layered Materials*; Lévy, F., Ed.; D. Reidel: Dordrecht, Holland, 1979; p 201.
(5) Subba Rao, G. V.; Shafer, M. W. In *Intercalated Layered Materials*; Lévy, F., Ed.; D. Reidel: Dordrecht, Holland, 1979; p 99.
(6) Friend, R. H.; Yoffe, A. B. *Adv. Phys.* **1989**, *36*, 1.
(7) Kortan, A. R.; Erbil, A.; Birgeneau, R. J.; Dresselhaus, M. S. *Phys. Rev. Lett.* **1982**, *49*, 1427.
(8) Winokur, M. J.; Clarke, R. *Phys. Rev. Lett.* **1985**, *54*, 811.
(9) Cowley, J. M.; Ibers, J. A. *Acta Crystallogr.* **1956**, *9*, 421.
(10) Hérold, A. In *Intercalated Layered Materials*; Lévy,F.; Ed.; D. Reidel: Dordrecht, Holland, 1979; p. 323.
(11) Dresselhaus, M. S.; Dresselhaus, G. in *Intercalated Layered Materials*; Lévy, F., Ed.; D. Reidel: Dordrecht, Holland, 1979; p 423.
(12) Ganal, P.; Moreau, P.; Ouvrard, G.; Sidorov, M.; McKelvy, M.; Glaunsinger, W. *Chem. Mater.* **1995**, *7*, 1132.
(13) Sidorov, M.; McKelvy, M.; Sharma, R.; Glaunsinger, W.; Ganal, P.; Moreau, P.; Ouvrard, G. *Chem. Mater.* **1995**, *7*, 1140.
(14) Atoji, M.; Schirber, J. E.; Swendson, C. A. *J. Chem. Phys.* **1959**, *31*, 1628.
(15) Brown, I. D.; Datars, W. R.; Gillespie, R. J.; Morgan, K. R.; Tun, Z.; Ummat, P. K. *J. Solid State Chem.* **1985**, *57*, 34.

0020-1669/95/1334-5496$09.00/0

pure Ta foils of 15 μm thickness and 99.95% pure sulfur in slight excess (≈3%). Sealed quartz ampules were heated to 1193 K with a temperature gradient over the ampules of about 100 K. After 4 days the ampules either were quenched into water (to retain the 1T-modification) or were sequentially annealed at 1073, 873, and 773 K.[18,19] The obtained samples were handled under inert conditions, since exposure of the host to air would inhibit Hg intercalation. In the case of β-$Hg_{1.3}TaS_2$, a slight Hg excess ($x > 1.3$) was used in order to ensure complete intercalation, whereas an exact ratio of Hg to TaS_2 (1.19:1.0) was used for α-$Hg_{1.19}TaS_2$. The latter samples were subsequently tempered at 473 K for 4 days, as ambient-temperature intercalation favors the formation of β-$Hg_{1.3}TaS_2$. During the annealing process, some of the added Hg usually condensed at the colder end of the glass tube. Thus, thermogravimetric analysis (TGA) and weight measurements of the added and recovered materials inherently yielded slightly lower compositions, $x = 1.13(3)$, than the maximum Hg uptake allowed by the α-$Hg_{1.19}TaS_2$ crystal structure.[18,19]

Suitable TEM samples were obtained by crushing the polycrystalline Hg intercalates under liquid nitrogen in an agate mortar. The resulting crystal fragments were then warmed to ambient temperature and dispersed onto holey carbon grids attached to a Gatan double-tilt liquid-nitrogen-cooled specimen holder. In combination with an built-in heating system, the latter device allowed direct temperature control between 100 and 373 K. The quality and homogeneity of our TEM samples were checked routinely by X-ray powder diffraction (XPD), both before and after the grinding process.

TEM measurements were made using a Philips CM30 transmission electron microscope (300 kV; spherical aberration coefficient (C_s) 2 mm; point-to-point resolution 0.23 nm). Due to the easy reversibility of the Hg intercalation process, all Hg_xTaS_2 samples inherently started to deintercalate Hg when exposed to the microscope vacuum at ambient or slightly elevated temperatures. Hence, we preferentially worked at low temperatures (typically 100 K) and weak beam intensities. These experimental conditions prevent the studied phases from noticeable mercury loss during data recording. It has been shown on parent titanium disulfide intercalated samples that, at room temperature, deintercalation may affect mercury content up to 20%.[13] This deintercalation appears mainly on crystallite edges, and if these areas are avoided, HRTEM data can be very well correlated to the X-ray diffraction structural information. We may then consider that the data obtained at a much lower temperature are very characteristic of the α and β phases with sample compositions very close to the nominal ones. The recorded diffraction patterns were calibrated using 2H-TaS_2 and Si as diffraction standards.

Results

The investigated TEM samples consisted of thin, platelike crystal fragments with either no distinct form or a hexagonal shape. These crystals were mainly oriented with their layers perpendicular to the electron beam as expected for a lamellar material. Unlike the case for $Hg_{1.24}TiS_2$, no tilting of the crystal specimens was required in order to align the **c** axis, suggesting that, in TaS_2 mercury intercalates, the **c** axis is perpendicular to the layers. Selected area diffraction (SAD) and micro diffraction (MD) photographs have been recorded for a large number of crystals covering a wide range of thicknesses and distances from the crystal edge. Special care was taken to avoid regions where the occurrence of visible black and white contrasts in the bright field images indicated an inhomogeneous Hg distribution (e.g. a Hg guest island formation).

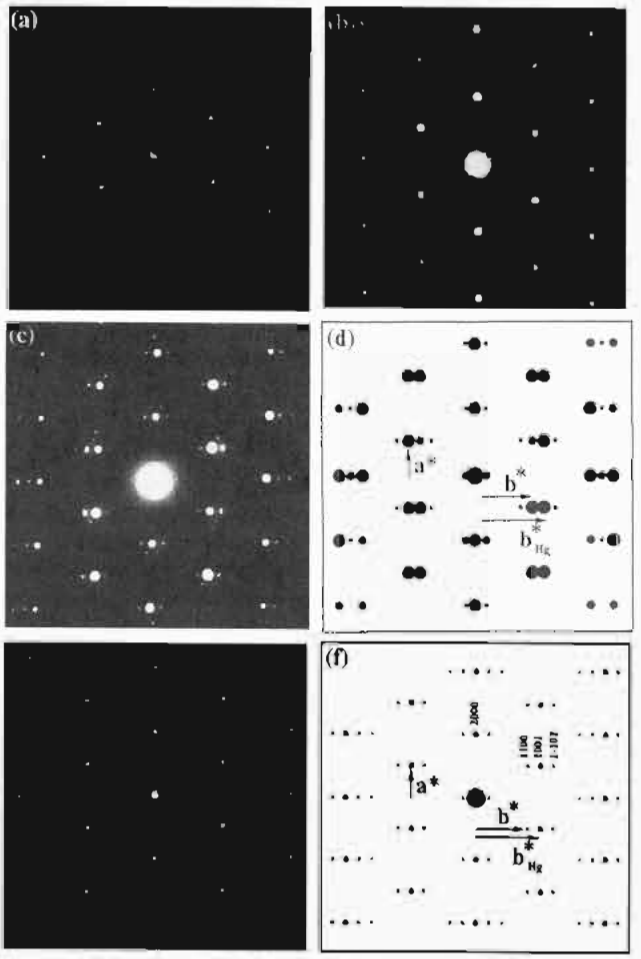

Figure 1. Typical micro diffraction (MD) patterns of (a) α-$Hg_{1.19}TaS_2$ (2H) and (c) α-$Hg_{1.19}TaS_2$ (1T) obtained along the c axis. (1T) and (2H) refer to the TaS_2 polymorph (either 2H-TaS_2 or 1T-TaS_2) used as starting material. (b) MD patterns obtained along the **c** axis for 2H-TaS_2 and (e) the structurally related mercury intercalation compound $Hg_{1.24}TiS_2$. (d) Computer simulation[20] of the α-$Hg_{1.19}TaS_2$ (1T) diffraction pattern based on the assumption of a (3+1) dimensional composite crystal structure and the layer stacking shown in Figure 5. As in the case of $Hg_{1.24}TiS_2$, the diffraction pattern can be indexed using the (3+1)-dimensional vector expression $\mathbf{H} = h\mathbf{a}^* + k\mathbf{b}^* + l\mathbf{c}^* + m\mathbf{b}^*_{Hg}$. In order to account for the double-diffraction spots in the experimental pattern (c), dynamic diffraction theory has been used. The best match with the experimental data has been obtained for crystal thicknesses in the order of 50 Å. (f) A schematic representation of the $Hg_{1.24}TiS_2$ MD pattern shown in (e). As indicated by the arrows, the TiS_2 host lattice and the Hg sublattice share a common **a*** axis but are incommensurate along the **b*** axis. The more intense reflections (large filled circles) can be easily associated with the Hg sublattice according to the large difference in scattering power.

α-$Hg_{1.19}TaS_2$. A typical (*hk*0) MD pattern of α-$Hg_{1.19}TaS_2$ (2H)[25] is shown in Figure 1a. The diffraction pattern consists of an inner set of hexagonal reflections at a corresponding *d*-spacing of 3.32(1) Å, which can easily be attributed to the TaS_2 sublattice, e.g. by comparison with the (*hk*0) pattern of pristine 2H-TaS_2 (Figure 1b). Each TaS_2 sublattice reflection is accompanied by two neighboring Hg sublattice reflections at 2.79 Å such that a characteristic triangular arrangement results. The positions of the Hg sublattice reflections are rotated by ±4° with respect to the TaS_2 host lattice. Their relative intensities varied, depending on the crystal thickness and the selected area, though most often they were found to be more or less equal. An extreme case is shown in Figure 1c, representing the (*hk*0) pattern of α-$Hg_{1.19}TaS_2$ (1T). Note that, with respect to the positions of the diffraction spots, the (*hk*0) patterns shown in Figure 1a and in Figure 1c are identical. However, the

(16) Ganal, P.; Olberding, W.; Butz, T.; Ouvrard, G. In *Chemical Physics of Intercalation II*; Bernier, P., Fischer, J. E., Roth, S., Solin, S. A., Eds.; NATO ASI Series B Vol. 305; Plenum Press: New York, 1993; p 383.
(17) Moreau, P.; Ouvrard, G. In *Chemical Physics of Intercalation II*; Bernier, P., Fischer, J. E., Roth, S., Solin, S. A., Eds.; NATO ASI Series B Vol. 305, Plenum Press: New York, 1993; p 351.
(18) Moreau, P. Ph.D. Thesis, University of Nantes, 1994.
(19) Ganal, P.; Moreau, P.; Ouvrard, G.; Olberding, W.; Butz, T. *Phys. Rev. B*, in press.

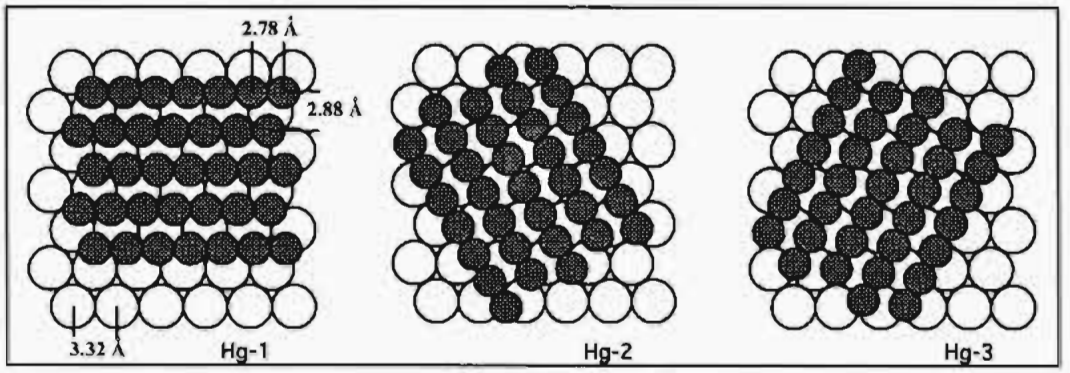

Figure 2. Model of the in-plane Hg structure of α-$Hg_{1.19}TaS_2$ viewed perpendicular to the layers. The Hg layers are composed of infinite chains of atoms aligned midway between neighboring sulfur rows. The 3-fold rotation symmetry exhibited by the TaS_2 host layers allows the formation of three equivalent orientation variants of Hg chains with respect to the TaS_2 host lattice. The different Hg sublattice domains usually occupy different guest galleries. The majority of investigated crystals contained all three Hg domains with about equal fractions, leading to the pseudohexagonal diffraction pattern shown in Figure 1a.

diffraction pattern in Figure 1c is dominated by a single subset of the Hg reflections, whereas the other subsets are less intense. In addition, second-order satellite reflections appear which can be attributed to double diffraction arising from the mutual alignment of the Hg guest and the TaS_2 host lattice. In total, the diffraction pattern bears a strong resemblance to that of $Hg_{1.24}TiS_2$ shown in Figure 1e.

According to reasoning similar to that used in the case of $Hg_{1.24}TiS_2$, the (*hk*0) pattern can be decomposed into two subsets of reflections that are indexed separately assuming *C*-face centered rectangular sublattices. These sublattices share a common **a*** axis but are incommensurate along the **b*** axis, as depicted schematically in Figure 1d,f. Since the commensurability along the **c*** axis is implied by the fact that the Hg guest and the TaS_2 host layers do not penetrate each other, a complete integer indexation of the whole diffraction pattern is thus possible with the (3+1)-dimensional vector expression $\mathbf{H} = h\mathbf{a}^* + k\mathbf{b}^* + l\mathbf{c}^* + m\mathbf{b}^*_{Hg}$.

If, as indicated by our TEM observations, the *c* axis is perpendicular to the layers, the MD patterns are consistent with two interpenetrating *C*-face centered orthorhombic sublattices and the in-plane lattice parameters of $a = 5.78(1)$ Å, $b = 3.32(1)$ Å, and $b_{Hg} = 2.78(1)$ Å. The indexation of the TEM diffraction patterns and the deduced lattice parameters are in perfect agreement with a recent XPD study[19] which quoted lattice parameters of $a = 5.757(2)$ Å, $b = 3.318(1)$ Å, $b_{Hg} = 2.781(1)$ Å, $c = 8.910(1)$ Å and $a = 5.765(1)$ Å, $b = 3.309(1)$ Å, $b_{Hg} = 2.782(1)$ Å, $c = 17.842(1)$ Å for α-$Hg_{1.19}TaS_2$ derived from 1T-TaS_2 and 2H-TaS_2, respectively. Note that in agreement with our TEM observations, α-$Hg_{1.19}TaS_2$ prepared from 1T-TaS_2 and 2H-TaS_2 exhibits the same in-plane layer arrangement. The structural differences between these compounds are limited to slightly different lattice parameters and, in the case of α-$Hg_{1.19}TaS_2$ (2H), to a doubling of the *c* parameter due to a different TaS_2 host layer stacking.

The lattice parameters of the Hg guest layer suggest a chainlike Hg arrangement (Figure 2a). The shortest Hg−Hg distance of 2.78 Å found along the incommensurate **b** axis is by far smaller than the next nearest interchain Hg−Hg distance of 3.20 Å, corresponding to a chain separation of 2.88 Å. There are three possibilities to align these chains with respect to the TaS_2 sublattice because of the 3-fold rotation symmetry exhibited by the undistorted TaS_2 host layers. Thus three symmetry-related Hg domains can be formed upon intercalation, as is depicted schematically in Figure 2. These domains may eventually coexist within the same host vdW gap. However, due to the strain energy associated with domain boundaries, it is, in general, more likely that they are formed in different guest galleries. Evidence for the presence of different Hg sublattice domains were found in all investigated crystals. However, their relative fractions varied significantly depending on the thickness of the crystals and the pristine material used for the preparation of α-$Hg_{1.19}TaS_2$. In the case of 1T-TaS_2, one Hg domain was predominant whereas, for 2H-TaS_2, usually all domains occurred with about equal probability, leading to the pseudohexagonal symmetry exhibited by the diffraction pattern in Figure 1a.

β-$Hg_{1.3}TaS_2$. SAD and micro diffraction patterns of β-$Hg_{1.3}TaS_2$ taken along the [001] zone axis exhibited a more or less hexagonal array of diffraction spots as is shown in Figure 3a. The diffraction pattern can be indexed using a hexagonal lattice and an *a* parameter of 5.8 Å. Alternatively one may consider the hexagonal TaS_2 host layers ($a = 3.32$ Å) as a 2×2 superstructure formed upon hexagonal closed packed Hg layers ($a_{Hg} = 2.90$ Å) (Figure 3d). Thus the β-$Hg_{1.3}TaS_2$ crystal structure would account for a maximum Hg uptake of $x = 4/3$, in good agreement with recent DSC and TGA studies.[18]

Kinematic scattering from such an arrangement does, as shown in Figure 3b, account for the bright spots in the diffraction pattern, but cannot explain the appearance of the weaker satellite reflections. The latter should be systematically absent due to the hexagonal symmetry exhibited by both the TaS_2 host and the Hg guest layers. However, the extinction condition is removed if dynamic diffraction is taken into account. Computer simulations[20] of the TEM diffraction pattern showed that, due to the high scattering power of the involved Hg and Ta atoms, multiple scattering already becomes important for crystals with a thickness of more than two layers. The intensity of the satellite reflections depends also on the phase shift between the Hg and the TaS_2 sublattices. Assuming that the unit cell contains a single Hg guest and TaS_2 host layer, the best match with the experimental data has been obtained with the Hg sublattice origin located on top of a sulfur atom, as illustrated in Figure 3d. Such a phasing of the Hg sublattice would provide linear and rectangular sulfur environments for the intercalated Hg atoms.

Although the idea of a commensurate Hg sublattice is overall consistent with the TEM data, it does not account for the more precise XPD patterns.[19] The *a* parameter of Hg sublattice deduced from the XPD data is found to be about 0.06 Å larger than expected from the commensurability condition. In addition, the XPD diagrams exhibit some unindexed reflections which

(20) O'Keefe, M. A.; Kilaas, R. NCEMSS: A program for the simulation of HRTEM Images. *Scanning Microsc. Suppl.* **1988**, *2*, 225.

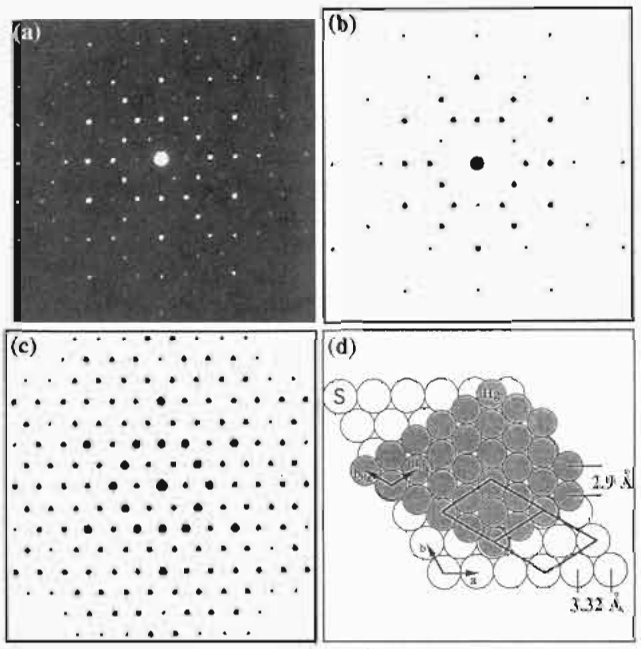

Figure 3. (a) Typical SAD pattern of β-$Hg_{1.3}TaS_2$ taken along the c axis. (b–c) Computer simulations[20] of the diffraction pattern based on dynamic diffraction theory and the in-plane structure model illustrated in (d). The calculated diffraction patterns in (b) and (c) are for specimens of 10 and 30 Å thicknesses, respectively. Note, that the inner set of reflection satellites is caused by double diffraction from the TaS_2 host and the Hg guest sublattice. Within the limits of the kinematic approximation (e.g., for a thin crystal as shown in Figure 4a) these reflections are systematically absent according to the hexagonal symmetry exhibited by both the TaS_2 layers and the Hg guest layers. (d) Model of the in-plane structure of β-$Hg_{1.3}TaS_2$ viewed perpendicular to the layers. The intercalated Hg atoms form a hexagonal compact guest layer with an in-plane Hg–Hg distance of 2.9 Å. The principal axes of the Hg guest layer are rotated by 30° with respect to the TaS_2 host lattice. Thus the TaS_2 host layers may be considered as a 2×2 superstructure formed upon hexagonal closed packed Hg layers.

are probably related to the occurrence of a monoclinic distortion within the Hg sublattice. Evidence for this also occurs in the TEM diffraction patterns. The SAD and MD patterns of all investigated crystals exhibited a slight but noticeable elliptical deformation.

Phase Transitions upon Hg Deintercalation. When exposed to the microscope vacuum at ambient or slightly elevated temperatures, all samples inherently started to deintercalate Hg. In order to demonstrate this in a more quantitative way, we deliberately heated a β-$Hg_{1.3}TaS_2$ crystal to 373 K and recorded MD patterns in regular time intervals. At this temperature, the β-$Hg_{1.3}TaS_2$ diffraction pattern (Figure 4a) gradually disappeared while, at the same time, the characteristic triangular reflection pattern of α-$Hg_{1.19}TaS_2$ appeared (Figure 4b). Upon further exposure to the microscope vacuum, the intensities of the Hg sublattice reflections diminished and we finally obtained the same pattern as for pristine 2H-TaS_2.

Discussion

The recorded diffraction patterns of α-$Hg_{1.19}TaS_2$ suggest that in this phase a chainlike Hg structure is realized in the TaS_2 vdW gap (Figure 2). The Hg chains form an ordered sublattice that shares two commensurate axes with the TaS_2 host matrix but is incommensurate along the Hg chain direction. The maximum Hg uptake allowed by the crystal structure is determined by the misfit between the TaS_2 host lattice and Hg sublattice and given by $x = b/b_{Hg} = 1.19$. This value is slightly larger than the maximum Hg uptakes ($x \approx 1.13(3)$) determined

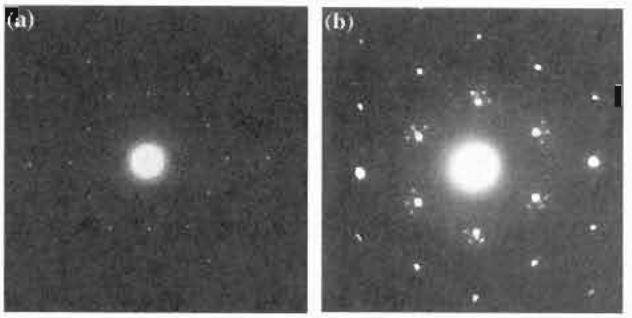

Figure 4. SAD patterns of a β-$Hg_{1.3}TaS_2$ (2H) crystal obtained at 373 K along the c axis. The SAD photographs were taken from the same area (a) immediately after heating the sample to 373 K and (b) after 1 h at this temperature. When exposed to the microscope vacuum at room temperature or slightly elevated temperatures, all samples inherently started to deintercalate Hg. At 373 K the diffraction pattern of β-$Hg_{1.3}TaS_2$ gradually disappeared while, at the same time, the triangular arrangement of reflection spot characteristic for α-$Hg_{1.19}TaS_2$ appeared.

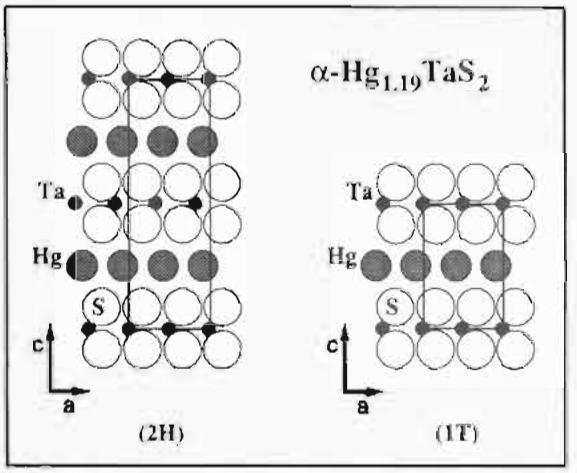

Figure 5. Schematic illustration of the principal stacking models proposed for the α-$Hg_{1.19}TaS_2$ crystal structure. The illustrations represent projections along the **b** axis showing the interlayer structure viewed parallel to the Hg chains. The proposed stacking models are based on the assumption that, in analogy to the $Hg_{1.24}TiS_2$ crystal structure, the incommensurate Hg chains are embedded into trigonal prismatic sulfur channels. Complementary XPD studies[18,19] indicated that both stacking variants might be realized, depending on the TaS_2 polymorph (2H-TaS_2 or 1T-TaS_2) used starting material.

by TGA studies.[18] However, it seems possible that the discrepancy might be related to the occurrence of Hg vacancies, which could be an intrinsic feature of the structure.[18,19]

If, in analogy to $Hg_{1.24}TiS_2$, the Hg chains are embedded into trigonal prismatic sulfur channels, then only the two principal stacking possibilities illustrated in Figure 5 remain. Complementary XPD studies indicated that both stackings might be realized, depending on the TaS_2 polymorph used as starting material.[19] Note that in both cases the Ta atoms are in a trigonal prismatic sulfur environment. The two stacking schemes differ only in the relative orientation of the TaS_2 layers. Compared to the structures of the pristine host materials, this requires in both cases a $\pm 1/3\ a$ glide shift along the orthorhombic **a** axis. However, the shear transformations affect in the case of 2H-TaS_2 every second TaS_2 slab, whereas in the case of 1T-TaS_2 every second sulfur layer is shifted.[19]

The observed intrachain Hg–Hg distance of 2.78 Å is typical for compounds containing polymercury cations (Hg_2Cl_2, $Hg_{2.94}AsF_6$, etc.)[15,21,22] and suggests the presence of a strong,

(21) Cutforth, B. D.; Davies, C. G.; Dean, P. A. W.; Gillespie, R. J.; Ireland, P. R.; Ummat, P. K. *Inorg. Chem.* **1973**, *12*, 1343.

metallic guest−guest interaction. This idea is further reinforced by the striking resemblance that the intercalated Hg layers share with β-Hg, a high-pressure phase of solid mercury.[14] The (101) lattice planes of the latter phase are, with respect to symmetry and bond lengths (2.825 and 3.158 Å), comparable to the intercalated Hg layers (2.78 and 3.20 Å). Obviously this analogy implies the formation of similar Hg metal bonds. Band structure calculations based on the extended Hückel theory confirmed that the electron orbitals of the intercalated Hg atoms exhibit a strong sp hybridization along the Hg-chain axis.[18] The σ-bond formed between the two nearest Hg neighbor atoms turned out to be slightly stronger than that in β-Hg whereas, on the other hand, the interaction between the neighboring Hg chains was somewhat reduced. Qualitatively, this is consistent with the slightly shorter intrachain bond length and the somewhat larger interchain distance. The great similarity between the Hg arrangement in α-$Hg_{1.19}TaS_2$ and β-Hg implies further that the interaction between the TaS_2 host matrix and the Hg guest layers has about the same order of magnitude as the interaction between neighboring Hg layers in β-Hg. The latter interaction is, however, identical to the interchain interaction because of the tetragonal symmetry of the β-Hg crystal structure. Thus, in perfect support of the general theory about misfit layer compounds, the unusual composite crystal structure adopted by α-$Hg_{1.19}TaS_2$ can be explained by the dominance of the Hg guest−guest interaction over a much weaker guest−host interaction.

In contrast to the Hg_xTiS_2 system, where, whatever the formal Hg uptake, only the chainlike Hg arrangement is realized, a second stage 1 compound, β-$Hg_{1.3}TaS_2$, is obtained upon mercuration of TaS_2. In this phase, the intercalated Hg atoms form a hexagonal compact metal sheet with an a parameter of 2.9 Å. Similar hexagonal Hg arrangements and bond lengths have been reported so far only for Hg_3MF_6 (M = Ta, Nb)[15] and, with reservations, for α-Hg.[23] In its usual solid state phase, each Hg atom encounters six nearest neighbors at a 3.006 Å distance located on the edges of a distorted octahedron. Perpendicular to the **c** axis, the next nearest Hg atoms form a hexagonal Hg layer with a Hg−Hg distance of 3.474 Å. Again, the quite comparable Hg−Hg bond lengths clearly underscore the importance of Hg−Hg metal bonding in the Hg intercalation compounds presented. It might also be illustrative to compare our results with the ternary $KHgC_8$ GIC compound.[24] There the Hg atoms are located on a buckled honeycomb net with an interatomic Hg−Hg distance of 2.84 Å. The Hg sublattice is sandwiched between two hexagonal K layers such that the K atoms are located above and below the center of each Hg honeycomb. If the K pair is substituted mentally by a Hg atom, this situation bears some resemblance to the proposed 2 × 2 superstructure: the suggested phasing of the Hg sublattice would result in two inequivalent Hg sites with linear and rectangular sulfur coordinations, respectively. As in the case of $KHgC_8$, the rectangular Hg sites would form a honeycomb network whose centers are occupied by linearly coordinated Hg atoms.

β-$Hg_{1.3}TaS_2$ is quite stable at room temperature and in the presence of excess of Hg. However, it slowly transforms to the α-phase when exposed to the microscope vacuum. Our in-situ TEM studies of the deintercalation process as well as a detailed XPD analysis of the Hg_xTaS_2 system ($x = 0.25-1.3$)[18] indicated that, besides the chainlike Hg structure in α-$Hg_{1.19}TaS_2$ and the hexagonal arrangement realized in β-$Hg_{1.3}TaS_2$, no other in-plane structures are possible. Lower formal Hg uptakes usually resulted in phase mixtures and/or random staging. This observation is not a surprise, since any other Hg arrangement would imply the breaking of the fairly strong Hg−Hg metal bonds. The fact that the hexagonal Hg arrangement is possible in the Hg_xTaS_2 system but not for Hg_xTiS_2 is probably related to the a parameter values of the TDM host lattice. In the case of TaS_2, the a parameter is such that the hexagonal Hg metal layer falls close to a 2 × 2 superstructure. Thus it seems likely that local commensurability with the host lattice (DC model) helps to stabilize this structure. Preliminary investigations of the Hg_xNbS_2 system, which has a comparable a parameter value, also indicate that two stage 1 compounds exist.[18]

Summary and Outlook

Hg intercalation into TaS_2 results in the formation of two stage 1 compounds. The in-plane Hg guest layer arrangements of these two compounds bear a strong resemblance to the Hg arrangements realized in the solid state phases of metallic Hg itself. Thus the unusually complex misfit structures exhibited by these intercalation compounds can be related to the competition between the strong Hg−Hg bonds and the weak guest−host interactions due to covalent Hg−S bonding. The intercalated Hg layers may in many respects be regarded as a frozen liquid with the usual Hg phase diagram modified by the lower dimensionality and the presence of Hg−S bonding. This idea is reinforced by the observation of Hg sublattice melting transitions at slightly higher temperatures.[18]

Acknowledgment. It is our pleasure to thank Prof. J. Rouxel for his continuous interest and support. This work was supported by a Human Capital and Mobility EC grant (P.G.).

IC950447M

(22) Cutforth, B. D.; Gillespie, R. J.; Ireland, P. R.; Sawyer, J. F.; Ummat, P. K. *Inorg. Chem.* **1983**, *22*, 1344.
(23) Grosse, A. V. *J. Inorg. Nucl. Chem.* **1965**, *27*, 773.
(24) Kertez, M.; Guloy, A. M. *Inorg. Chem.* **1987**, *26*, 2852.
(25) The addition (2H) or (1T) denotes the TaS_2 polymorph that has been used as starting material. Although α-$Hg_{1.19}TaS_2$ samples derived from 1T-TaS_2 and 2H-TaS_2, respectively, exhibit overall the same structure features, they differ slightly in the stacking of the TaS_2 slabs.[18,19]